Electrical and magnetic properties of hexagonal $BaTiO_{3-\delta}$

T. Kolodiazhnyi*
ICYS, National Institute for Materials Science, 1-1 Namiki, Tsukuba, Ibaraki 305-0044, Japan

A. A. Belik
ANML, National Institute for Materials Science, 1-1 Namiki, Tsukuba, Ibaraki 305-0044, Japan

S. C. Wimbush
Department of Materials Science and Metallurgy, University of Cambridge, Pembroke Street, Cambridge CB2 3QZ, United Kingdom

H. Haneda
SMC, National Institute for Materials Science, 1-1 Namiki, Tsukuba, Ibaraki 305-0044, Japan

(Received 12 September 2007; revised manuscript received 14 November 2007; published 5 February 2008)

The electrical resistivity, Hall coefficient, and magnetic susceptibility of *n*-type hexagonal $BaTiO_{3-\delta}$ (hex-$BaTiO_{3-\delta}$) have been measured in the 5–400 K temperature range. Above 200 K this compound undergoes a transition from an insulating to a semiconducting state. Below 140 K Hall effect data indicate the existence of an energy gap of approximately 43 meV separating the localized electron ground state from the conduction band. Magnetic measurements reveal a strong magnetic anomaly in hex-$BaTiO_{3-\delta}$ with a maximum in the susceptibility at around 160–200 K. This anomaly is quite similar to that of the hexagonal $BaMg_{1/3}Ru_{2/3}O_3$ which may indicate that the electron ground state in hex-$BaTiO_{3-\delta}$ is comprised of spin singlet Ti^{3+}-Ti^{3+} dimers. We further propose that the thermal dissociation of these dimers is responsible for the change in the electron transport mechanism in hex-$BaTiO_{3-\delta}$.

DOI: 10.1103/PhysRevB.77.075103 PACS number(s): 77.84.Dy, 71.38.Ht, 71.38.Mx

I. INTRODUCTION

$BaTiO_3$ exists in two polymorphs, the perovskite and a hexagonal form. The high-temperature hexagonal structure (denoted here as hex-$BaTiO_3$) can be stabilized by partial substitution of Ti with Mn, Fe, Sc, or Cr compensated by oxygen vacancies.[1] Alternatively, doping with oxygen vacancies alone can also transform perovskite $BaTiO_3$ into hexagonal form when the concentration of the O vacancies approaches 1–2 at. %.[2] In the latter case the charge compensation of the oxygen vacancies is achieved by electrons. Although there are no available electronic band calculations of hex-$BaTiO_{3-\delta}$, it can reasonably be assumed that the compensating electrons reside on the Ti 3*d* orbitals, thus rendering the material *n*-type.

The hex-$BaTiO_3$ structure ($P6_3/mmc$ space group) can be viewed as a Ti_2O_9 dimer comprising two face-sharing TiO_6 octahedra interconnected with six corner-sharing TiO_6 octahedra. As a result, there are two nonequivalent sites for the Ti ions, located within the corner-sharing and face-sharing oxygen octahedra. Similar to the Ti ions, the O ions also have two nonequivalent crystallographic sites in hex-$BaTiO_3$. According to the high resolution neutron diffraction study reported by Sinclair *et al.*,[3] O vacancies in hex-$BaTiO_{3-\delta}$ reside exclusively on the hexagonal $BaO_{3-\delta}$ layers separating the two face-sharing oxygen octahedra. The presence of oxygen vacancies in hex-$BaTiO_{3-\delta}$ may have important implications for the electronic properties of this compound. However, except for some resistivity data obtained on hex-$BaTiO_{2.88}$ ceramic,[3] little is known about the electronic and magnetic properties of hex-$BaTiO_{3-\delta}$.

In this contribution we report on the electrical resistivity, Hall coefficient, and magnetic susceptibility of both multidomain single crystal and sintered ceramic hex-$BaTiO_{3-\delta}$ measured in the 5–400 K temperature range. Magnetic measurements reveal a strong magnetic anomaly in hex-$BaTiO_{3-\delta}$ which, we believe, is directly related to the electron transport mechanism in this compound. We attribute this magnetic anomaly to the random dimerization of the Ti^{3+} ions which form a magnetically silent ground state. The driving force behind this dimerization is not yet clear but might be both the antiferromagnetic exchange interaction between neighboring Ti^{3+} ions and the phonon-assisted formation of static small bipolarons.

II. EXPERIMENT

Both ceramics and single crystals of hex-$BaTiO_{3-\delta}$ have been studied. Multidomain single crystals of hex-$BaTiO_{3-\delta}$ were obtained by careful reduction of perovskite $BaTiO_3$ single crystals in forming gas (3% H_2/97% N_2) at 1350 °C. Polycrystalline ceramic hex-$BaTiO_{3-\delta}$ samples were prepared by solid state reaction of high purity (99.999%) $BaCO_3$ and TiO_2 powders sourced from Sigma-Aldrich. To achieve different levels of reduction, ceramics denoted C1 and C2 were sintered at 1360 °C in the forming gas at a flow rate of 20 and 100 cm^3/min, respectively. An insulating hexagonal ceramic denoted C0 was obtained from C1 by oxidation in air at 800 °C for 20 h. The phase purity of both the single crystal and the ceramics was examined by x-ray diffraction and scanning electronic microscope (SEM) energy-dispersive x-ray (EDX) microanalysis. Lattice parameters were obtained from Rietveld refinement of the x-ray data obtained at room temperature on a Rigaku Ultima III x-ray diffractometer ($\lambda = 0.154\,06$ nm). Electrical resistivity, Hall effect, and magnetic susceptibility were measured on a

 ©2008 The American Physical Society

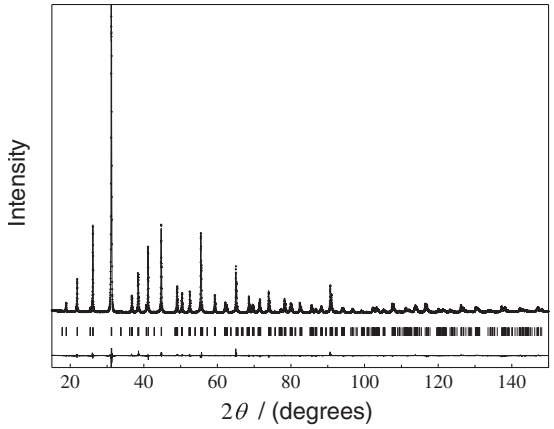

FIG. 1. Room-temperature x-ray diffraction pattern of sample C1 (+). Calculated diffraction pattern from Rietveld refinement of hex-$BaTiO_3$ (solid line). The vertical bars indicate the positions of expected Bragg peaks. The difference between observed and calculated data is shown at the bottom of the plot.

Quantum Design Physical Property Measurement System (PPMS) and Magnetic Property Measurement System (MPMS).

III. RESULTS

Room-temperature x-ray diffraction patterns of hex-$BaTiO_{3-\delta}$ show no evidence of secondary phases. To extract the lattice parameters of the samples, the initial atomic coordinates and lattice parameters were set to the values reported by Akimoto *et al.*[4] for hex-$BaTiO_3$ and refined based on the $P6_3/mmc$ space group. By way of example, the refinement of the pattern of ceramic sample C1 is shown in Fig. 1. The refined lattice parameters for the hex-$BaTiO_{3-\delta}$ samples studied here along with room-temperature electron concentrations obtained from the Hall effect measurements are given in Table I.

The resolution of the x-ray data obtained on a laboratory x-ray diffractometer did not allow us to accurately refine the O-site occupancy. Although the lattice parameters of reduced samples do not show a clear correlation with electron concentration, they are always larger than those of the oxygenated sample, in general agreement with the neutron diffraction data.[3]

TABLE I. Lattice parameters a and c, and electron concentrations n at 300 K for ceramic samples C0 (fully oxygenated), C1 (reduced), and C2 (more reduced), and single crystal sample SC. The pattern (R_p) and weighted pattern (R_{wp}) are reliability factors of the Rietveld refinement.

Parameter	C0	C1	SC	C2
a (nm)	0.57252	0.57319	0.57313	0.57309
c (nm)	1.39681	1.39882	1.39903	1.39850
R_p (%)	7.73	5.96	14.01	9.00
R_{wp} (%)	11.14	8.38	17.43	12.86
n (cm^{-3})	$<1\times10^{12}$	7.9×10^{19}	1.7×10^{20}	2.3×10^{20}

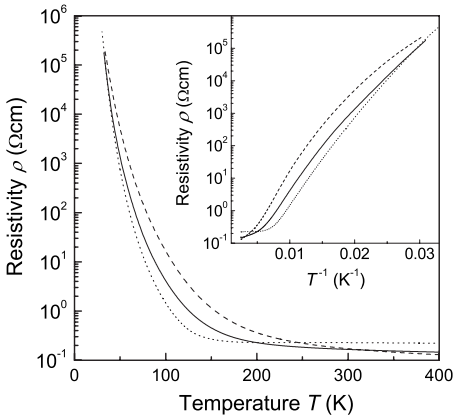

FIG. 2. Electrical resistivity of the hex-$BaTiO_{3-\delta}$ single crystal (solid line), C1 ceramic (dotted line), and C2 ceramic (dashed line) as a function of temperature. The inset shows an Arrhenius plot of the resistivity as a function of $1/T$ for the same samples.

Each oxygen atom removed from the hex-$BaTiO_3$ lattice by reduction leaves behind an O vacancy and two electrons. The physical nature of these electrons has been explored by electrical resistivity, Hall effect, and magnetic susceptibility measurements described below.

The temperature dependences of the electrical resistivity ρ of the hex-$BaTiO_{3-\delta}$ single crystal and C1 and C2 ceramics are shown in Fig. 2. The $\rho(T)$ of both the single crystal and the ceramics shows qualitatively similar features with a broad sample-dependent transition from the insulating to semiconducting $\rho(T)$ behavior above 200 K. This transition is seen more clearly in the inset of Fig. 2 where ρ is plotted as a function of the reciprocal temperature. In the 200–400 K interval the resistivity shows semiconductor-type behavior. It slowly decreases with T although the $\rho(T)$ dependence is quite weak with resistivity values in the range of 0.1–0.3 Ω cm. We note, however, that the $\rho(T)$ dependence in the 200–400 K range is sample dependent and becomes steeper with increasing degree of reduction of the sample. Upon cooling below 200 K, ρ increases strongly indicating an insulating ground state. Based on both our data and the data reported for strongly reduced hex-$BaTiO_{2.88}$ ceramic,[3] it is obvious that the transition in the $\rho(T)$ behavior in hex-$BaTiO_{3-\delta}$ is a universal feature which occurs over a broad range of electron doping from 7.9×10^{19} to 3.5×10^{21} cm^{-3} examined so far.

As demonstrated in the inset of Fig. 2, below 100 K $\rho(T)$ shows a significant downturn which does not agree with a simple Arrhenius-type behavior. This deviation becomes more pronounced in the samples having a higher degree of reduction. Sinclair *et al.*[3] demonstrated that the $\rho(T)$ dependence of their hex-$BaTiO_{2.88}$ ceramic below 160 K can be well fitted with a variable range hopping (VRH) model [i.e., $\ln(\rho) \propto T^{-1/4}$]. In order to find out whether the VRH model applies also to our weakly doped samples, we fit a similar functional dependence [$\ln(\rho) \propto T^{-m}$] to our data. As revealed in Fig. 3, we were not able to fit the data with a fixed $m=1/4$ value. Instead, the m decreases from 0.67 for sample C1 to 0.20 for sample C2 as the degree of the reduction of

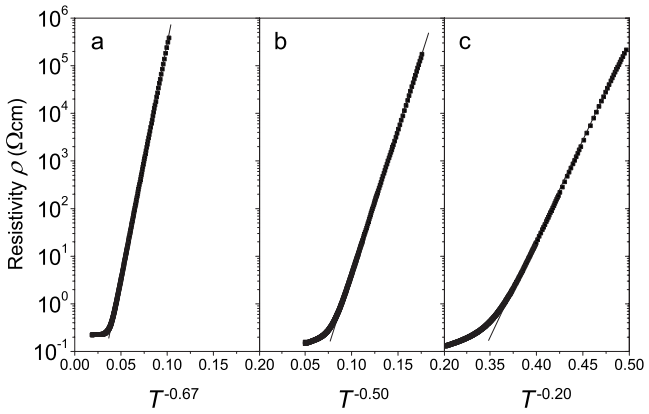

FIG. 3. The best linear fit of the low-temperature part of the electrical resistivity of the hex-$BaTiO_{3-\delta}$ samples as a function of T^{-m}. (a) C1 ceramic $m=0.67$; (b) single crystal $m=0.50$; (c) C2 ceramic $m=0.20$.

the hex-$BaTiO_{3-\delta}$ samples increases. This behavior is inconsistent with the VRH model which assumes a constant $m=1/4$ for three-dimensional hopping. Although our results do not support the VRH model in the case of the weakly doped samples, it may still be possible that this model can apply in the heavily reduced hex-$BaTiO_{2.88}$ ceramic studied by Sinclair *et al.*[3] High concentration of the oxygen vacancies in the latter sample may introduce substantial lattice disorder which would create a finite density of localized electron states within the band gap. Below the mobility edge, the phonon-assisted hopping of the charge carriers via these localized states would result in VRH. Nevertheless, for weakly reduced samples we suggest that there must be another reason for the non-Arrhenius-type $\rho(T)$ behavior than that suggested in Ref. 3. For example, the complex $\rho(T)$ dependence may be the result of a temperature-dependent concentration $n(T)$ and mobility $\mu(T)$ of the charge carriers.

The temperature dependence of the charge carrier concentration was investigated by Hall effect measurements. The sign of the Hall coefficient R_H was negative throughout the studied temperature interval thus confirming that the charge carriers are electrons. The Hall coefficient data presented in Fig. 4 for both ceramics and the single crystal indicate that below 150 K the concentration of the charge carriers ($n=1/eR_H$) has a clear activation behavior with $E_H \approx 43$ meV. Above 170 K, $R_H(T)$ shows strong dependence on the sample preparation condition. Similar to the $\rho(T)$ behavior, the slope of R_H vs $1/T$ above 170 K increases with the degree of reduction of the samples.

The Hall mobility of the charge carriers, μ_H, was calculated from the ρ and R_H data ($\mu_H=R_H/\rho$) and is shown in Fig. 5. Owing to the strong crystal anisotropy of hex-$BaTiO_3$ one should treat the absolute values of μ_H reported here with caution. However, the temperature dependence of μ_H is qualitatively similar for both the ceramics and the single crystal. Below 200 K the electron mobility increases with temperature which, together with the temperature-dependent concentration of the charge carriers, accounts for the deviation of the $\rho(T)$ from an Arrhenius-type behavior. A low-temperature increase in μ_H with T is typical for extrinsic

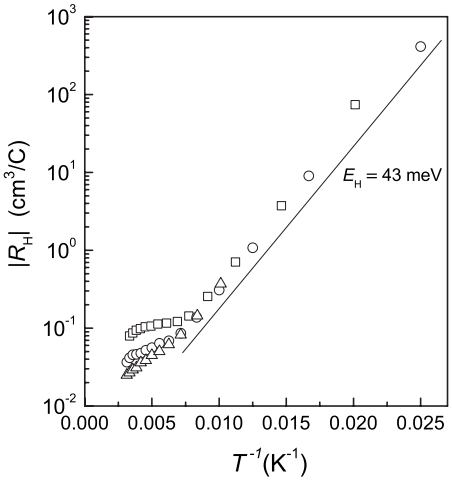

FIG. 4. Temperature dependence of the Hall coefficient of the C1 ceramic (squares), single crystal (circles), and C2 ceramic (triangles). The solid line indicates an activation energy of 43 meV.

semiconductors where electrons are scattered on the shallow donorlike impurities. As a consequence, the μ_H of hex-$BaTiO_{3-\delta}$ shows a strong dependence on the degree of reduction of the sample. Samples with lower electron concentrations show higher values of μ_H. As will be shown below, these donorlike impurities are Ti^{3+} and [Ti^{3+}-Ti^{3+}] defects. With increasing temperature the concentration of the electrons localized on Ti ions decreases which results in the increase in the Hall mobility with T. At high enough T, most of the impurities are ionized and the mobility reaches its maximum and starts to decrease due to electron-phonon scattering.

To get further insight into the electronic properties of hex-$BaTiO_{3-\delta}$ we performed magnetic susceptibility, χ, measurements at 7 T as a function of temperature. The results are shown in Fig. 6. The insulating hex-$BaTiO_3$ ceramic (C0) shows a temperature-independent diamagnetic susceptibility ($\chi \approx -2.37 \times 10^{-5}$ cm^3/mol). A central result of this paper is

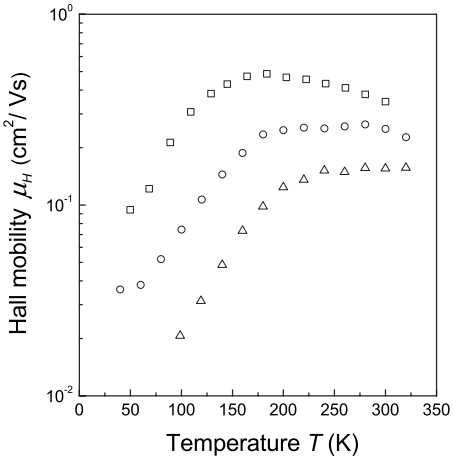

FIG. 5. Temperature dependence of the Hall mobility of electrons in C1 ceramic (squares), single crystal (circles), and C2 ceramic (triangles).

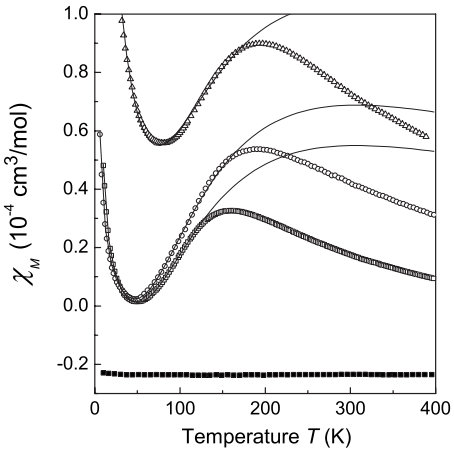

FIG. 6. Molar magnetic susceptibility of C0 ceramic (solid squares), C1 ceramic (open squares), single crystal (circles), and C2 ceramic (triangles). Solid lines are fits to the low-temperature data as described in the text.

an anomalous χ behavior with a $\chi(T)$ maximum at 160–180 K which develops in the electron doped hex-$BaTiO_{3-\delta}$ samples as the doping level is increased. The anomaly is rather broad and can be attributed to electronic rather than crystallographic changes. The magnitude of the anomaly increases with the degree of reduction of the samples. In contrast to the fully oxygenated C0 sample, the electron-doped ceramics show a noticeable upturn in χ below 60 K due to the presence of the paramagnetic ions. Since the undoped C0 sample shows a very weak low-temperature paramagnetic tail, the presence of any significant amount of extrinsic paramagnetic impurities in the samples can be ruled out. Hence the only paramagnetic ion responsible for the low-temperature upturn of χ in hex-$BaTiO_{3-\delta}$ is Ti^{3+}.[5]

Since hex-$BaTiO_{3-\delta}$ has an insulating electron ground state, we initially assume that at low temperature all doped electrons must be localized on the Ti ions. To determine the concentration of the doped electrons trapped at the isolated Ti^{3+} ions we have fitted the low-temperature part ($T<60$ K) of the $\chi(T)$ dependence with the Curie law given by

$$\chi_p = \frac{N_A p^2 \mu_B^2 c_{Ti^{3+}}}{3k_B T}, \tag{1}$$

where N_A is the Avogadro number, $p=1.73$ is the effective magnetic moment of Ti^{3+} in Bohr magnetons (μ_B), k_B is the Boltzmann constant, T is the temperature, and $c_{Ti^{3+}}$ is the concentration of Ti^{3+}.

By comparison of the concentration of doped electrons given in Table I and the $c_{Ti^{3+}}$ listed in Table II it appears that less than 10% of the doped electrons are localized on the isolated Ti^{3+} at low T. Why are the rest of the Ti^{3+} ions magnetically "silent"? The answer to this question lies in the anomalous $\chi(T)$ behavior above 60 K. In fact, a number of titanates, such as Ti_4O_7 ($3d^{0.5}$), Na(Li)$TiSi_2O_6$ ($3d^1$), $MgTi_2O_4$ ($3d^1$), TiOCl ($3d^1$), and $LiTi_2O_4$ ($3d^{0.5}$), demonstrate a similar magnetic anomaly indicative of systems having a spin singlet ground state.[6–8] Dimerization of the Ti^{3+} ions in the aforementioned compounds is held responsible for the $\chi(T)$ behavior. In all these cases, the $\chi(T)$ anomaly is also accompanied by crystallographic and metal-insulator transitions (with the exception of $LiTi_2O_4$, which is a superconductor below 12.4 K), as itinerant electrons freeze into static electron dimers, chains, and more complex superstructures.[9]

TABLE II. Fitting parameters for the fits to the magnetic susceptibility data.

	C1	SC	C2
$c_{Ti^{3+}}$ (cm^{-3})	2.04×10^{18}	1.95×10^{19}	1.44×10^{19}
χ_0 (cm^3/mol)	-1.1×10^{-5}	-9.7×10^{-6}	-4.1×10^{-6}
Δ (meV)	27.1	26.9	29.3
C_0 (cm^3 K/mol)	5.5×10^{-2}	6.6×10^{-2}	8.9×10^{-2}

The main difference between the above mentioned titanates and the hex-$BaTiO_{3-\delta}$ studied here is that in the former compounds the concentration of the Ti^{3+} ions is quite high, $3d^{0.5}$ or $3d^1$. In other words either half or all of the Ti lattice sites are occupied by the Ti^{3+} ions. In contrast, in the case of the hex-$BaTiO_{3-\delta}$ studied here the concentration of the Ti^{3+} ions is very low, $3d^{0.001}$–$3d^{0.01}$, and any magnetic phase separation with long-range magnetic ordering is unlikely. Moreover, the magnetic anomaly in hex-$BaTiO_{3-\delta}$ is rather broad which strongly suggests that it does not originate from the crystallographic phase transition. The absence of any long-range magnetic order has been also confirmed by neutron diffraction studies of hex-$BaTiO_{2.88}$ ($3d^{0.24}$) at 4 K.[3] Therefore we propose that the magnetic anomaly in hex-$BaTiO_{3-\delta}$ is associated with the formation of *random* [Ti^{3+}-Ti^{3+}] dimers with a spin singlet ($S=0$) ground state. Thermal activation of these $S=0$ dimers to a triplet state ($S=1$) as well as their thermal dissociation into isolated Ti^{3+} ($S=1/2$) states explains very well the $\chi(T)$ dependence above 60 K. Moreover, it is then obvious that the crossover from insulating to semiconducting behavior in hex-$BaTiO_{3-\delta}$ arises as a natural consequence of this process.

By extrapolating the low- and high-temperature resistivity data (inset in Fig. 2) we can follow a shift in the crossover temperature from insulating to semiconducting behavior of hex-$BaTiO_{3-\delta}$ as the n increases. The crossover temperatures are 137, 170, and 198 K for C1, SC, and C2 samples, respectively. We can also see a shift in the crossover temperature in the Hall mobility data in Fig. 5. By utilizing a similar extrapolation procedure, we determine the crossover temperatures to be 145, 168, and 197 K for C1, SC, and C2 samples, respectively. The crossover temperatures determined from the $\chi(T)$ data are 138, 162, and 181 K for C1, SC, and C2 samples, respectively. Bearing in mind that these data were obtained from three independent experiments the correspondence in the crossover temperatures estimated by these methods is quite remarkable.

It is quite interesting to compare our data with the results on the $BaMg_{1/3}Ru_{2/3}O_3$ compound with the identical ($P6_3/mmc$ space group, $a=5.765$ Å, $c=14.13$ Å) hexagonal structure.[10] In this compound the Ru^{5+} ions are ordered into

$S=0$ [Ru^{5+}-Ru^{5+}] pairs in the Ru_2O_9 clusters and interact strongly through antiferromagnetic exchange. Thermal excitations of the [Ru^{5+}-Ru^{5+}] singlet to the $S=1$, 2, and 3 states give rise to a magnetic anomaly similar to that seen in hex-$BaTiO_{3-\delta}$. However, unlike in hex-$BaTiO_{3-\delta}$, thermally excited electrons cannot "hop" to the neighboring (Mg^{2+}) ion and remain within the Ru_2O_9 cluster which explains the high activation energy of the resistivity of the $BaMg_{1/3}Ru_{2/3}O_3$ compound.[10]

In view of the strong electron-phonon interaction in titanium compounds, one would expect at least two main contributions to the binding energy of the [Ti^{3+}-Ti^{3+}] dimer: one from the magnetic superexchange interaction which favors an antiferromagnetic spin configuration on the neighboring Ti^{3+} ions and one from the electron-phonon interaction which may also cause the localization of the [Ti^{3+}-Ti^{3+}] dimer in a form of a small bipolaron. Unfortunately we are not aware of any comprehensive theory that treats the problem of the random electron dimers by explicitly taking into account both spin-spin and electron-phonon interactions. Recently we have applied Emin's model of singlet small bipolarons[11] to explain the magnetic anomaly in Nb-doped $BaTiO_3$ perovskite.[12] However, it should be stressed here that Emin's model accounts only for the electron-lattice interaction in the formation of the intersite electron dimer.

Therefore to estimate the energy of the magnetic interaction of the [Ti^{3+}-Ti^{3+}] dimer, Δ, we followed the approach proposed by Taniguchi *et al.*[13] for the quasi-two-dimensional CaV_4O_9. The total magnetic susceptibility can be described as a sum of the low-temperature paramagnetic susceptibility χ_p, given by Eq. (1), the temperature independent diamagnetic and Van Vleck paramagnetic susceptibility, combined as χ_0, and the spin susceptibility χ_{spin}. According to Ref. 13, χ_{spin} at low temperatures ($k_BT \ll \Delta$) is given by

$$\chi_{spin} = C_0 T^{(d/2)-1} \exp\left(-\frac{\Delta}{k_B T}\right), \tag{2}$$

where C_0 is a sample-dependent constant and d is the dimensionality of the system. Since the random [Ti^{3+}-Ti^{3+}] dimers can be considered as zero-dimensional defects, we set $d=0$. The fit to the $\chi(T)$ data is shown as solid lines in Fig. 6 and the fitting parameters are given in Table II. A reasonably good fit was obtained for $T<150$ K which satisfies the $k_BT \ll \Delta$ condition. From this analysis we obtain the magnetic interaction energy Δ for both single crystal and ceramic samples to be in the range of 27–29 meV. By comparing this energy with the $E_H \approx 43$ meV obtained from the Hall data we conclude that the magnetic contribution accounts for about two-thirds of the total binding energy of the [Ti^{3+}-Ti^{3+}] dimer.

IV. CONCLUSIONS

Reduction of hex-$BaTiO_{3-\delta}$ in an oxygen deficient atmosphere is an effective method to dope it with electron charge carriers. The Hall mobility of charge carriers at high temperatures is rather low and is comparable with that of the perovskite $BaTiO_{3-\delta}$. Upon cooling, both the mobility and the conductivity of hex-$BaTiO_{3-\delta}$ decrease which indicates that the charge carriers become localized. Our resistivity and Hall effect data do not support the Anderson-type localization model in the weakly doped samples and suggest a true energy gap between a localized ground state and the conduction band. It can be reasonably assumed, however, that samples with a higher concentration of oxygen vacancies will have a significant degree of disorder. In this case one would expect that the electron transport at low temperatures will be governed by the disorder-induced Anderson localization as reported in Ref. 3 for heavily doped $BaTiO_{3-\delta}$ with $\delta=0.15$. We report a broad magnetic anomaly in hex-$BaTiO_{3-\delta}$. We propose that both the magnetic anomaly and the details of the $\rho(T)$ dependence in hex-$BaTiO_{3-\delta}$ be attributed to the formation of static spin singlet [Ti^{3+}-Ti^{3+}] dimers with a total binding energy of approximately 43 meV. Analysis of the magnetic susceptibility data suggests that about two-thirds of this energy is due to magnetic interactions. Furthermore, we argue that the [Ti^{3+}-Ti^{3+}] dimers form at random as there is no indication of long range order in the neutron diffraction data at 4 K.[3] The local crystallographic symmetry of the [Ti^{3+}-Ti^{3+}] dimers as well as isolated Ti^{3+} centers are currently being studied by electron paramagnetic resonance measurements and will be reported elsewhere.

ACKNOWLEDGMENTS

The authors are grateful to J. E. Greedan for useful comments. This study was performed using Special Coordination Funds for Promoting Science and Technology from the Ministry of Education, Culture, Sports, Science and Technology of the Japanese Government.

*kolodiazhnyi.taras@nims.go.jp

[1] A. Kirianov, N. Ozaki, H. Ohsato, N. Kohzu, and H. Kishi, Jpn. J. Appl. Phys., Part 1 **40**, 5619 (2001); I. E. Grey, C. Li, L. M. D. Cranswick, R. S. Roth, and T. A. Vanderah, J. Solid State Chem. **135**, 312 (1998).

[2] H. Arend and L. Kihlborg, J. Am. Ceram. Soc. **52**, 63 (1969).

[3] D. C. Sinclair, J. M. S. Skakle, F. D. Morrison, R. I. Smith, and T. P. Beales, J. Mater. Chem. **9**, 1327 (1999).

[4] J. Akimoto, Y. Gotoh, and Y. Oosawa, Acta Crystallogr., Sect. C: Cryst. Struct. Commun. **50**, 160 (1994).

[5] Below 70 K we detect a strong Ti^{3+} signal by electron paramagnetic resosnance. The details of the crystal symmetry of this paramagnetic defect will be reported elsewhere.

[6] S. Lakkis, C. Schlenker, B. K. Chakraverty, R. Buder, and M. Marezio, Phys. Rev. B **14**, 1429 (1976).

[7] M. Isobe, E. Ninomiya, A. N. Vasil'ev, and Y. Ueda, J. Phys. Soc. Jpn. **71**, 1423 (2002); M. Isobe and Y. Ueda, *ibid.* **71**, 1848 (2002); J. van Wezel and J. van den Brink, Europhys. Lett. **75**, 957 (2006).

[8] D. C. Johnston, H. Prakash, W. H. Zachariasen, and R. Viswanathan, Mater. Res. Bull. **8**, 777 (1973).
[9] D. I. Khomskii and T. Mizokawa, Phys. Rev. Lett. **94**, 156402 (2005).
[10] J. Darriet, M. Drillon, G. Villeneuve, and P. Hagenmuller, J. Solid State Chem. **19**, 213 (1976).
[11] D. Emin, Phys. Rev. B **53**, 1260 (1996).
[12] T. Kolodiazhnyi and S. C. Wimbush, Phys. Rev. Lett. **96**, 246404 (2006).
[13] S. Taniguchi, T. Nishikawa, Y. Yasui, Y. Kobayashi, M. Sato, T. Nishioka, M. Kontani, and K. Sano, J. Phys. Soc. Jpn. **63**, 4529 (1995).